



Nicotinic and Muscarinic Acetylcholine Receptor Agonists Counteract Cognitive Impairment in a Rat Model of Doxorubicin-Induced Chemobrain via Attenuation of Multiple Programmed Cell Death Pathways

Benjamin Ongnok^{1,2,3} · Nanthip Prathumsap^{2,3} · Titikorn Chunchai^{1,2,3} · Patcharapong Pantiya^{1,2,3} · Busarin Arunsak^{2,3} · Nipon Chattipakorn^{2,3} · Siriporn C. Chattipakorn^{1,2,3,4} 

Received: 1 August 2023 / Accepted: 21 March 2024

© The Author(s), under exclusive licence to Springer Science+Business Media, LLC, part of Springer Nature 2024

Abstract

Chemotherapy causes undesirable long-term neurological sequelae, chemotherapy-induced cognitive impairment (CICI), or chemobrain in cancer survivors. Activation of programmed cell death (PCD) has been proposed to implicate in the development and progression of chemobrain. Neuronal apoptosis has been extensively recognized in experimental models of chemobrain, but little is known about alternative forms of PCD in response to chemotherapy. Activation of acetylcholine receptors (AChRs) is emerging as a promising target in attenuating a wide variety of the neuronal death associated with neurodegeneration. Thus, this study aimed to investigate the therapeutic capacity of AChR agonists on cognitive function and molecular hallmarks of multiple PCD against chemotherapy neurotoxicity. To establish the chemobrain model, male Wistar rats were assigned to receive six doses of doxorubicin (DOX: 3 mg/kg) via intraperitoneal injection. The DOX-treated rats received either an $\alpha 7$ nAChR agonist (PNU-282987: 3 mg/kg/day), mAChR agonists (bethanechol: 12 mg/kg/day), or the two as a combined treatment. DOX administration led to impaired cognitive function via neuroinflammation, glial activation, reduced synaptic/blood–brain barrier integrity, defective mitochondrial ROS-detoxifying capacity, and dynamic imbalance. DOX insult also mediated hyperphosphorylation of Tau and simultaneously induced various PCD, including apoptosis, necroptosis, and pyroptosis in the hippocampus. Concomitant treatment with either PNU-282987, bethanechol, or a combination of the two potently attenuated neuroinflammation, mitochondrial dyshomeostasis, and Tau hyperphosphorylation, thereby suppressing excessive apoptosis, necroptosis, and pyroptosis and improving cognitive function in DOX-treated rats. Our findings suggest that activation of AChRs using their agonists effectively protected against DOX-induced neuronal death and chemobrain.

Keywords Chemotherapy · Chemobrain · Neurotoxicity · Doxorubicin · Acetylcholine receptor agonists

✉ Siriporn C. Chattipakorn
siriporn.c@cmu.ac.th; scchattipakorn@gmail.com

¹ Neuroelectrophysiology Unit, Cardiac Electrophysiology Research and Training Center, Faculty of Medicine, Chiang Mai University, Mueang Chiang Mai 50200, Chiang Mai, Thailand

² Center of Excellence in Cardiac Electrophysiology Research, Chiang Mai University, Mueang Chiang Mai 50200, Chiang Mai, Thailand

³ Cardiac Electrophysiology Unit, Department of Physiology, Chiang Mai University, Mueang Chiang Mai 50200, Chiang Mai, Thailand

⁴ Department of Oral Biology and Diagnostic Sciences, Faculty of Dentistry, Chiang Mai University, Mueang Chiang Mai 50200, Chiang Mai, Thailand

Introduction

Refinements in clinical diagnosis and advances in cancer treatment have contributed to tremendous improvement in cancer survival rates and outcomes in cancer patients [1]. Nonetheless, longitudinal studies have documented the emergence of cognitive deficits in approximately 19–78% of cancer survivors who underwent chemotherapy as part of their treatment regimen [2–5]. The debilitating neurological sequelae in several cognitive domains following chemotherapy have currently become well-recognized and colloquially referred to as chemobrain which sometimes can be long-lasting and have irreversible symptoms [6–8]. With an estimation of 70 million cancer survivors around the world

by the year 2020, understanding the pathological basis and findings of novel therapeutic approaches to treat chemobrain is urgent [9, 10].

Although doxorubicin (DOX) is a remarkable chemotherapeutic drug extensively used to treat various types of cancer, it has been well-documented that it causes chemobrain across patients with numerous types of cancer [11, 12]. Neuroinflammation and mitochondrial dysfunction have been proposed as crucial contributors to DOX-induced chemobrain [13–18]. The cross-link between these cellular candidates is an intricate pathophysiological threat, resulting in neuronal apoptosis, which is commonly acknowledged as the ultimate characteristic of DOX-induced chemobrain [13, 14]. Aberrant activation of alternative lytic pro-inflammatory programmed cell death (PCD) including necroptosis and pyroptosis has been recently observed in response to inflammatory processes, resulting in the impact of neuronal death and a vicious cycle of chronic neuroinflammation in certain specific brain regions [19]. These two types of PCD, distinct from apoptosis, have been shown to implicate the progression of neurodegenerative and neuroinflammatory disorders, contributing to the release of immunogenic cellular content and ultimately undesirable loss of neuronal cells and function [19, 20]. However, the contribution of PCD in response to chemotherapeutic agents is still inconclusive based on a very limited number of studies. Although various types of PCD including apoptosis, necroptosis, and pyroptosis, have been documented in experimental models of chemobrain [21–23], the molecular phenotypes of PCD have never been examined simultaneously in the same study model. Therefore, addressing the characteristics of the types of PCD underlying the pathophysiology of chemobrain possibly facilitates the development of better therapeutic interventions against chemobrain in cancer patients.

In addition to PCD, the potential Alzheimer's lesions and accelerated age-related tauopathy have been suggested as hallmarks of chemobrain pathology [21, 24, 25]. An elevation of Alzheimer's disease (AD) biomarkers, including Tau protein in the peripheral circulation has been observed in patients who received cancer treatments [26]. The physiologic functions of Tau in the brain are to facilitate the formation and stabilization of microtubules by adhering to microtubules, thereby enabling the axonal transport of cellular vesicles and organelles [27]. Notably, the pathological post-translational modification of Tau, especially of hyperphosphorylation, is mainly responsible for its loss of normal physiological function and gain of neurotoxicity, contributing to cognitive deterioration in patients with AD [27]. In this aspect, glycogen synthase kinase-3 (GSK3) is traditionally considered a constitutively active kinase implicated in the hyperphosphorylation of Tau. There are two isoforms of GSK3, GSK3- α , and GSK3 β [28]. GSK3 β is the most

ubiquitous, and it is found to be hyperactive in the brains of AD patients, providing empirical support that it contributes to AD pathogenesis through distinct mechanisms [28, 29]. Even though we have previously demonstrated that long-term administration of DOX led to the hyperphosphorylation of Tau at Thr181 [21], the molecular involvement of GSK3 β and hyperphosphorylation of Tau following chemotherapy has never been investigated.

The coordination of different cognitive functions, especially in hippocampus-dependent learning and memory, requires appropriate cholinergic signaling via the activation of acetylcholine receptors (AChRs) [30, 31]. Cholinergic hypofunction has been identified as one of the key consequences of AD; therefore, correspondingly, the cholinergic hypothesis of AD proposes that therapy targeting cholinergic enhancement could be useful in ameliorating cognitive decline [30]. Importantly, cholinergic modulation using AChR agonists has been shown to effectively alleviate the impairment of cognitive and behavioral performance induced by lesions of cholinergic circuitry or antagonism of cholinergic receptors [32–34]. Additionally, there is accumulating evidence to indicate the anti-inflammatory roles of cholinergic stimulation in the peripheral and central nervous system (CNS) through both muscarinic receptors (mAChR) and nicotinic receptors (nAChR), especially in the case of $\alpha 7$ subtype ($\alpha 7$ nAChR) [35–37]. However, several gaps of knowledge still exist since mechanistic insights regarding the effects of AChR agonists on inflammatory types of PCD and hyperphosphorylation of Tau following DOX administration have never been demonstrated. Therefore, the present study aimed to test the hypothesis that enhancing systemic cholinergic signaling with mAChR and $\alpha 7$ nAChR agonists provides neuroprotection against DOX-induced chemobrain via the reduction of mitochondrial dysfunction, neuroinflammation, hyperphosphorylation of Tau, and pro-inflammatory PCD, thereby improving hippocampal-dependent learning and memory.

Materials and Methods

Animal Model

Adult male Wistar rats ($n=40$, 350–400 g, 8-week-old) were sourced from the Nomura Siam International Co, Ltd., Thailand, and were maintained at the laboratory animal center of Chiangmai University in controlled conditions (21 ± 1 °C, $50 \pm 10\%$ humidity, 12-h light:dark cycle). All experimental procedures were conducted in accordance with a protocol authorized by the Institutional Animal Care and Use Committee (IACUC) of Chiang Mai University (permit no. 2563/RT-0012) and NIH recommendations (Guide for the Care and Use of Laboratory Animals).

Chemotherapy and Treatment Paradigms

After 1 week of acclimatization, all rats were divided into a control group ($n=8$) and a DOX-treated group ($n=32$) to receive six doses of either 0.9% NSS or 3 mg/kg of DOX (Fresenius Kabi Oncology Ltd., India) via intraperitoneal injection (i.p.). The sample size was calculated by using the G*Power program (version 3.1.9.4) according to our preliminary study. The initial three doses were administered every 4 days, followed by the final three doses administered once per week. The dosage and administration protocol of DOX in this study are determined based on our preliminary data, which indicates that this specific dose can induce cognitive impairments in rats. Furthermore, this dosage is comparable to those employed in our prior investigations [21, 38]. Rats in the DOX-treated group were subdivided into four groups ($n=8$ /groups) to be intraperitoneally treated with either 0.9% normal saline as the vehicle, PNU-282987 ($\alpha 7$ nAChR agonist; 3 mg/kg/day, Alomone, Israel) [39], bethanechol (mAChR agonist; 12 mg/kg/day, Sigma-Aldrich, USA) [40], or a combined administration of PNU-282987 and bethanechol for 30 consecutive days, starting

with the first dose of DOX injection. The dosages of PNU-282987 and bethanechol used were based on previous studies [39, 40]. Twenty-four hours following the administration of the last dose of all treatments, animals were cognitively assessed.

Behavioral Tests

After the completion of the treatment paradigm, all rats were subjected to a series of tests to assess cognitive function consisting of a novel object location task (NOLT) and a novel object recognition task (NORT) as illustrated in Fig. 1A. To confirm the results and impose a greater cognitive load on long-term learning and memory, the test scenario was modified so that the NOLT and NORT were conducted with a 24-h interval between each test [41, 42]. Briefly, rats were allowed to explore an arena (a 70-cm-diameter and 50-cm-height made of an opaque plastic tank) for 10 min during the habituation phase. The following day, rats were given 10 min to explore the testing arena containing two identical objects during the familiarization phase prior to being transferred back to their home cages for 24 h. In the NOLT phase, each rat was positioned in the center of an arena

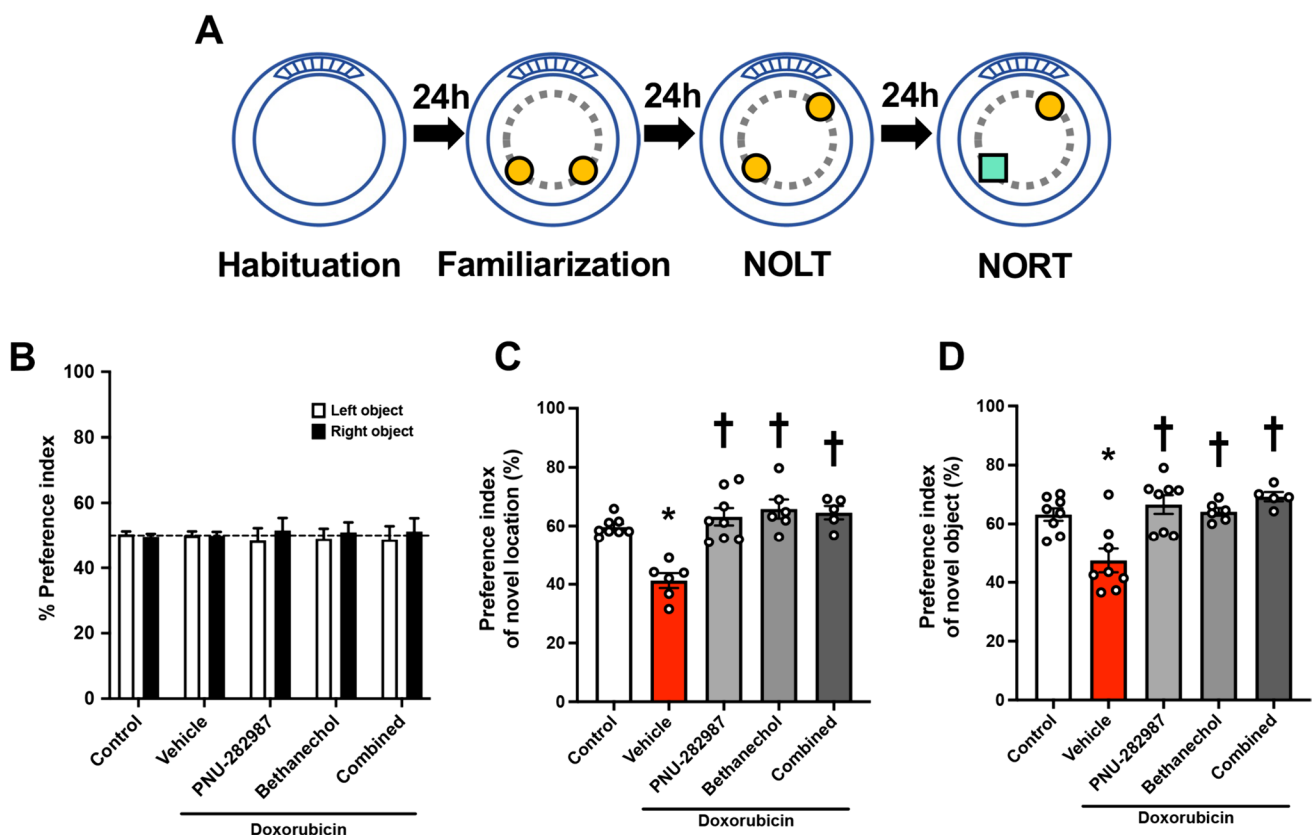


Fig. 1 The effects of an $\alpha 7$ nAChR agonist and mAChR agonist on cognitive function in DOX-induced chemobrain. **A** The behavioral test procedure. **B** The percentage preference index of two objects during the familiarization phase in the modified novel object location and recognition tests. **C** The percentage preference index of the

object in a novel location during the novel object location test. **D** The percentage preference index of a novel object during the novel object recognition test; $n=6-8$ /group; * $p<0.05$ vs. control; † $p<0.05$ vs. DOX + vehicle (one-way ANOVA followed by an LSD post hoc test). NOLT, novel object location test; NORT, novel object recognition test

containing the same two objects, one at the same location as in the familiarization phase and the other at the opposite end. The rats were given 10 min to explore the objects. The rats were returned to the arena 24 h after the NOLT, where one of the familiar objects at the novel location was replaced with a novel object. The percentage of preference indices for NOLT and NORT was calculated by dividing the amount of time the rat spent exploring the object at the novel location in NOLT or the novel object in NORT by the total amount of time spent exploring both objects during a 10-min testing period.

Western Blot Analysis

The hippocampal tissues were homogenized with an ice-cold non-ionizing lysis buffer containing 100 mM NaCl (RCI Labscan Limited., Thailand), 25 mM EDTA (Ajax Finechem™, Australia), 10 mM Tris (HiMedia Laboratories Pvt. Ltd., India), 1% *v/v* Triton X-100 (Sigma-Aldrich, USA), 1% *v/v* NP-40 (Thermo Fisher Scientific, USA), and 1× protease inhibitor (Merck KGaA, Germany). Equal amounts of protein at 30 µg were separated by 10% hand-casting SDS–polyacrylamide gel electrophoresis and transferred onto nitrocellulose membranes. Then, membranes were blocked for 1 h with 5% bovine serum albumin (BSA) or 5% non-fat dry milk Tris-buffered saline with 0.1% Tween buffer at room temperature for 1 h. They were then probed overnight at 4 °C with primary antibodies as shown in supplementary Table 1. All immunoblots were then probed with secondary antibodies conjugated with horseradish peroxidase as shown in supplementary Table 1 at room temperature for 1 h. Protein band immunoreactivities were detected using the ChemiDoc™ Touch Gel Imaging System (Bio-Rad Laboratories, USA).

Morphological Analysis of Microglia and Astrocytes

Prior to cryoprotection by immersion in 30% sucrose, the brains were postfixed in 4% paraformaldehyde (PFA) in PBS overnight. The brain tissues were sectioned with a cryostat (Leica CM1950, Leica, Germany) into 20-µm coronal sections. After 1 h in permeabilizing solution (3% H₂O₂ and 1% Triton X-100 in distilled water), sections were blocked in 5% BSA in PBS for 1 h. To label microglia and astrocytes, primary antibodies against goat anti-Iba-1 (1:1000 dilution; ab5076, Abcam, USA) and rabbit anti-GFAP (1:1000 dilution; ab16997, Abcam, USA) were applied to the brain slices, respectively. The sections were then rinsed three times and probed with Alexa Flour 488-labeled donkey anti-goat IgG (1:1000; ab150129, Abcam, USA) and Alexa Flour 647-labeled goat anti-rabbit IgG (1:500; ab150079, Abcam, USA) for 1 h, followed by nuclear staining with DAPI (TOCRIS, UK) for 15 min. The hippocampal CA1 region was imaged using 60× objectives with a confocal microscope (Olympus FLUOVIEW FV3000, Japan). Morphological

analyses of microglia and astrocytes were carried out utilizing Imaris software (Oxford Instruments) [43–46].

The Response of Brain Mitochondria to Oxidative Stress

After decapitation, the brains were rapidly removed and homogenized with 0.05% bacterial proteinase (Sigma-Aldrich, USA) in ice-cold MSE solution consisting of 25 mM mannitol (Elago Enterprises Pty Ltd., Australia), 75 mM sucrose (RCI Labscan Limited., Thailand), 1 mM EGTA (Sigma-Aldrich, USA), 5 mM HEPES (Sigma-Aldrich, USA), and 1 mg/ml BSA (HiMedia Laboratories Pvt. Ltd., India) at 600 rpm. Differential centrifugation was performed to isolate the mitochondrial fraction [18, 47]. The isolated mitochondrial fraction was stained with dichlorohydrofluorescein diacetate (DCFH-DA) dye (Sigma-Aldrich, USA) for 20 min at room temperature to measure the level of mitochondrial reactive oxygen species (ROS). To determine the change in mitochondrial membrane potential ($\Delta\Psi_m$), the isolated mitochondrial suspension was incubated with JC-1 dye (Sigma-Aldrich, USA) for 15 min at 37 °C. A reduction in the proportion of red to green fluorescence intensity indicates depolarization of $\Delta\Psi_m$. 2 mmol/L H₂O₂ was co-incubated with either DCFH-DA or JC-1 dye to ascertain the potential of mitochondria to neutralize ROS. The percentage change in emission intensity between mitochondria stimulated with and without H₂O₂ was evaluated. By measuring the absorbance of mitochondrial fraction at a wavelength of 540 nm, the swelling of mitochondria was determined [48]. A decrease in the absorbance signifies mitochondrial swelling. All mitochondrial studies were performed in triplicate.

Dendritic Spine Staining

The fresh brain tissues were glued onto a metal block holder and coronally sectioned to a thickness of 400 µm by using a vibrating blade microtome (Vibratome Series 1000 Sectioning system, UK). Brain sections were then fixed in 4% PFA for 1 h and stained for 7 days with DiI dye (Invitrogen, USA). The secondary or tertiary dendritic segments of three pyramidal neurons were captured from the CA1 region per section using a confocal microscope (Olympus FLUOVIEW FV3000, Japan). The density and volume of dendritic spines were evaluated as previously described [49].

Quantification and Statistical Analysis

Data administration and representation were carried out using GraphPad Prism software (version 7, GraphPad Software, Inc., USA). All error bars shown indicate the standard error of the mean (SEM). A one-way ANOVA followed by

an LSD post hoc test was performed to compare multiple groups. A p -value < 0.05 was considered a measure of statistical significance.

Results

AChR Agonists Attenuated Cognitive Dysfunction in Rats with DOX-Induced Chemobrain

To determine the therapeutic effects of parasympathetic activation on DOX-induced cognitive impairment, the NOLT and NORT were performed as shown in Fig. 1A. In this study, parasympathomimetic drugs including PNU-282987 and bethanechol were administered to activate the $\alpha 7$ nAChR and mAChR, respectively. There was no significant difference in the amount of time spent interacting with two objects among all groups in the familiarization phase, indicating no preference between the two objects (Fig. 1B). During the NOLT, DOX-treated rats exhibited cognitive impairment as evidenced by a substantial reduction in the preference index during the NOLT, compared to that of the controls (Fig. 1C). Interestingly, PNU-282987, bethanechol, and the combined treatment equally improved the preference index in the NOLT (Fig. 1C). Consistent with the NOLT, DOX administration shortened the time interaction with the new object in the NORT (Fig. 1D). Noticeably, PNU-282987, bethanechol, or the two as a combined treatment substantially prolonged the time rats spent interacting with the novel object. These findings showed that PNU-282987, bethanechol, and the combined drugs equally prevented cognitive deficits in rats treated with DOX.

The $\alpha 7$ nAChR Agonist and mAChR Agonist Maintained the Density and Volume of Dendritic Spines, Enhanced the Levels of Tight Junction Proteins, and Mitigated Hyperphosphorylation of Tau in Rats with DOX-Induced Chemobrain

The dendritic spine density/volume and the expression level of PSD-95 were then examined to determine dendritic spine density and volume as represented in Fig. 2A–E. Fluorescence analysis demonstrated that the number and volume of dendritic spines were remarkably reduced in DOX-treated rats compared with the controls (Fig. 2A–C). Consistent with these findings, the expression level of PSD-95 was also markedly reduced in the DOX-treated group, suggesting synaptic dysplasticity following DOX treatment (Fig. 2D, E). In particular, long-term treatment with PNU-282987, bethanechol, and the combined drugs effectively preserved dendritic spine density, spine volume, and PSD-95 expression in DOX-treated rats (Fig. 2A–E). Furthermore, the expression levels of tight junction proteins including claudin-5 and occludin in the hippocampus were substantially decreased in DOX-treated rats

relative to the control group (Fig. 2D, F, G), implying weakening BBB integrity. Critically, the activation of $\alpha 7$ nAChR and mAChR led to a significant upregulation of hippocampal tight junction proteins to the levels observed in the control group (Fig. 2D, F). The combined therapy of both AChR agonists contributed a similar outcome as either as a monotherapy (Fig. 2D, F, G). In addition, DOX administration resulted in hyperphosphorylation of Tau at Thr181, a well-established pathological feature of AD (Fig. 2D, I). Given that GSK3 β is a key kinase enzyme responsible for the phosphorylation of Tau, which was inactivated by phosphorylation at Ser9, we subsequently investigated the phosphorylation level of GSK3 β at Ser9 in the hippocampal tissues. The results demonstrated that there were no detectable alterations in the phosphorylation of GSK3 β at Ser9 between the control and DOX groups (Fig. 2D, H). However, PNU-282987, bethanechol, or the two as a combined treatment ameliorated the hyperphosphorylation of Tau and augmented the phosphorylated GSK3 β at Ser9 in DOX-treated rats, suggesting that activation of the AChR axis mediates the suppressed phosphorylation of Tau via the inactivation of GSK3 β (Fig. 2D, H, I).

Activation of AChRs Mitigated the Hippocampal Inflammation Induced by DOX in Rats

In contrast to the control group, DOX-treated rats exhibited neuroinflammation in the hippocampus as evidenced by increases in the phosphorylation of NF- κ B at Ser536 and the expression of TNF- α (Fig. 3A–C). Consistently, DOX administration reduced the expression level of IL-10 and the phosphorylation of STAT3 at Tyr705, compared with the controls (Fig. 3A, C, D). Treatment with AChR agonists, either PNU-282987 or bethanechol, effectively counteracted these upregulated pro-inflammatory markers and increased the expression of IL-10 relative to those observed in rats treated with DOX alone (Fig. 3A–E). Notably, a substantial increase in the phosphorylation of STAT3 at Tyr705 was observed in rats treated with PNU-282987 and the combined treatment in comparison to the DOX-treated rats receiving the vehicle (Fig. 3A–E), suggesting that activation of $\alpha 7$ nAChR, but not mAChR, effectively induced STAT3 anti-inflammatory signaling. Taken together, this suggested that activation of $\alpha 7$ nAChR and mAChR attenuated neuroinflammation in the hippocampus of rats with DOX-induced chemobrain.

The $\alpha 7$ nAChR Agonist and mAChR Agonist Preserved the Morphologies of Microglia and Astrocytes in the Hippocampus of Rats with DOX-Induced Chemobrain

To investigate the modulatory effects of cholinergic activation on microglial reactivity, microglial morphology at the hippocampal CA1 region was further determined as shown

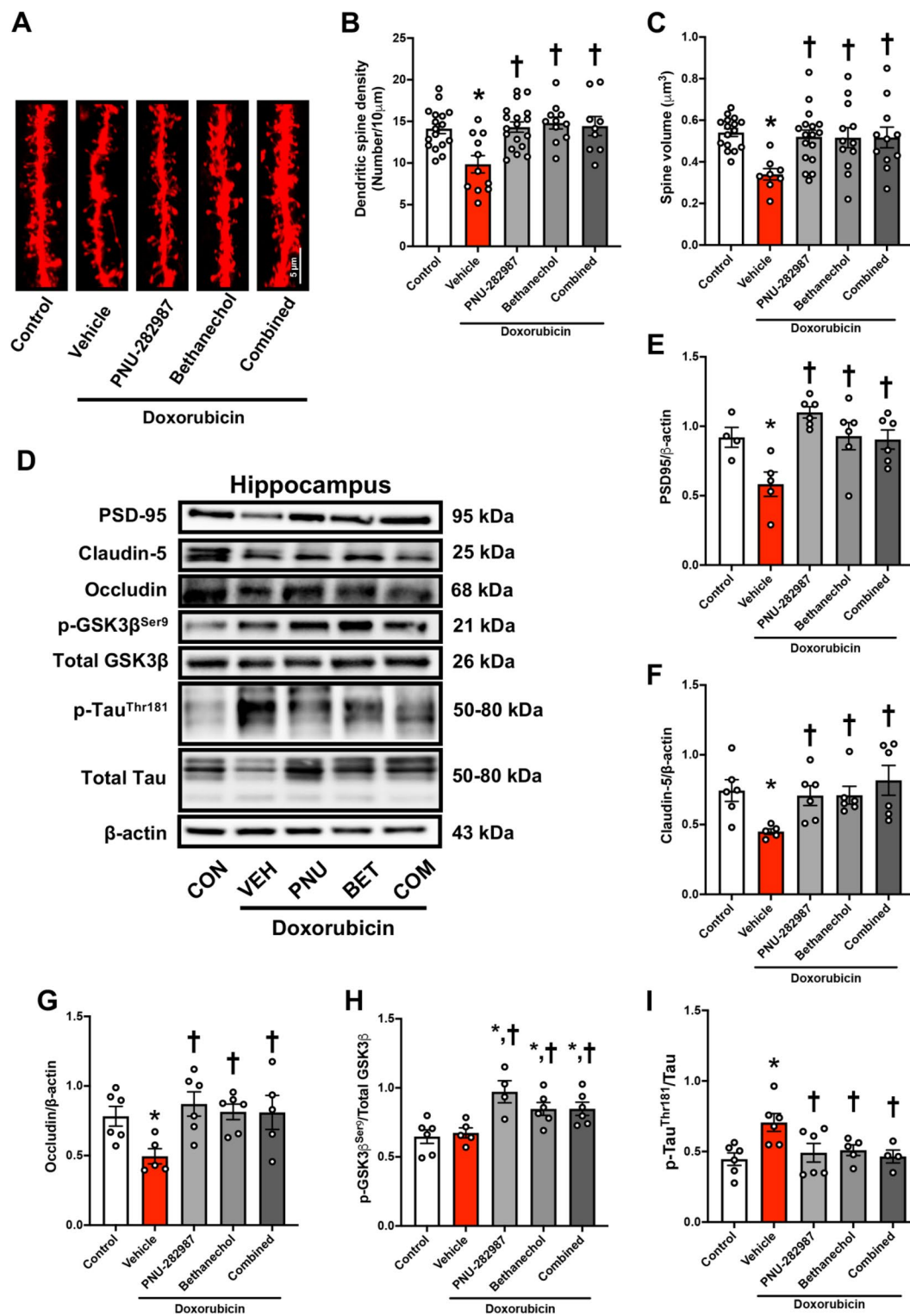
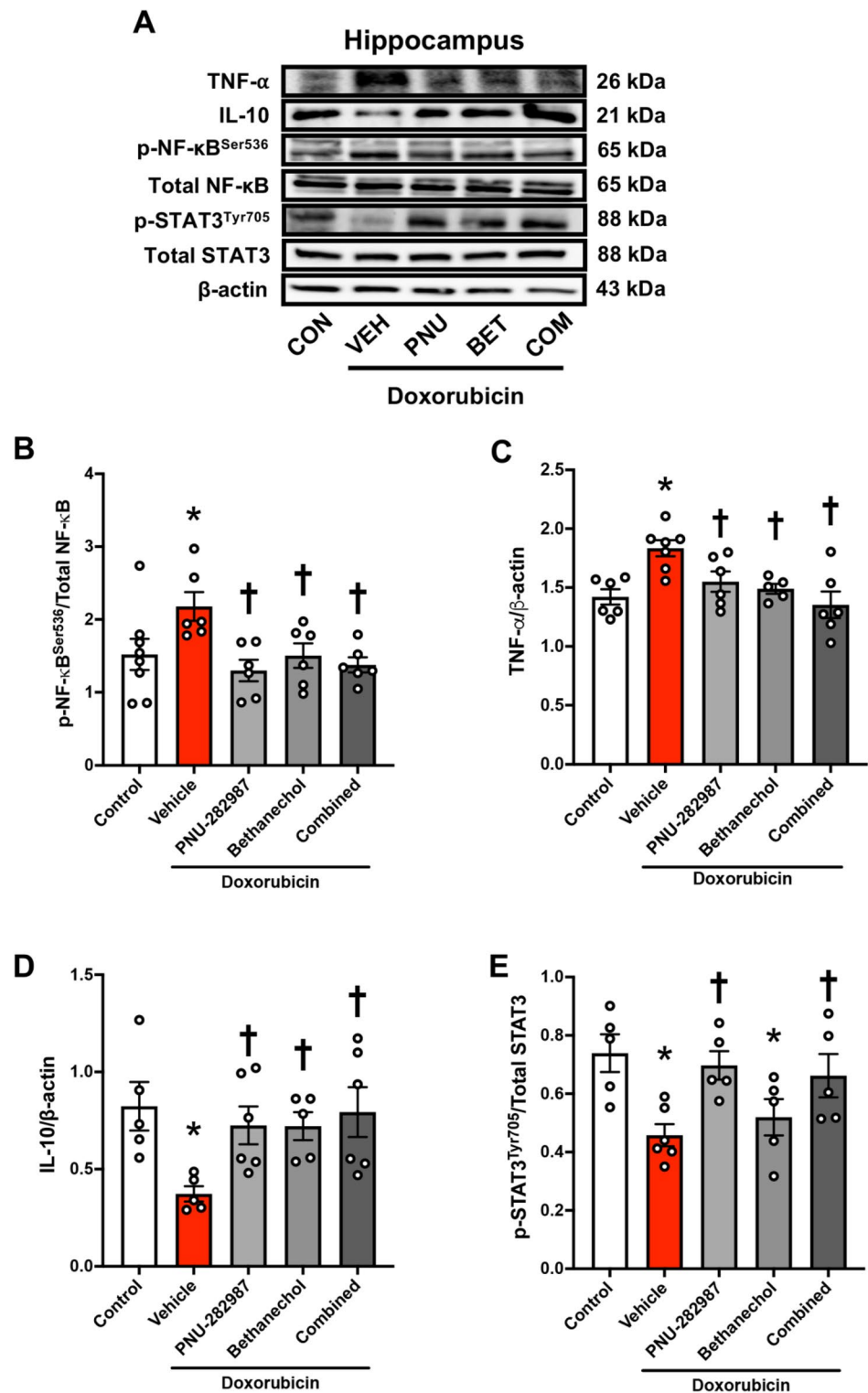


Fig. 2 The effects of an $\alpha 7$ nAChR agonist and mAChR agonist on dendritic spines, tight-junction protein expressions, and tau phosphorylation in rats with DOX-induced chemobrain. **A** Representative images of dendritic spine density using DiI staining. **B** The number of dendritic spines per 10- μ m apical tertiary dendrite. **C** Dendritic spine volume. **D** Representative western blot bands. **E** PSD-95 protein expression. **F** Claudin-5 protein expression. **G** Occludin protein

expression. **H** The expression ratio of p-GSK3 β ^{Ser9}/total GSK3 β . **I** The expression ratio of p-Tau^{Thr181}/total Tau; $n=12$ slices from six rats/group for DiI staining and $n=4-6$ /group for western blotting; $*p < 0.05$ vs. control; $\dagger p < 0.05$ vs. DOX + vehicle (one-way ANOVA followed by an LSD post hoc test). GSK3 β , glycogen synthase kinase-3 β ; PSD-95, postsynaptic density protein 95

Fig. 3 The effects of $\alpha 7$ nAChR agonist and mAChR agonist on hippocampal inflammation in rats with DOX-induced chemobrain. **A** Representative western blot bands. **B** The expression ratio of p-NF- κ B^{Ser536}/total NF- κ B. **C** TNF- α protein expression. **D** IL-10 protein expression. **E** The expression ratio of p-STAT3^{Tyr705}/total STAT3. $n = 4-6$ /group; * $p < 0.05$ vs. control; † $p < 0.05$ vs. DOX + vehicle (one-way ANOVA followed by an LSD post hoc test)



in Fig. 4A. Fluorescence analysis revealed that DOX-treated rats exhibited microglial activation as indicated by increases in the number of Iba-1⁺ cells, Iba-1 immunofluorescence intensity, and soma volume of Iba-1⁺ cells (Fig. 4A–D). Microglial filament analysis was then performed, and the outcomes are illustrated in Fig. 4E. Administration of

DOX reduced the length and branching of microglial processes (Fig. 4F–H), implying that DOX treatment caused a change in microglial morphology to an amoeboid-shaped neurotoxic phenotype. Remarkably, long-term treatments with $\alpha 7$ nAChR, mAChR, and combined agonists in DOX-treated rats maintained all aspects of microglial morphology

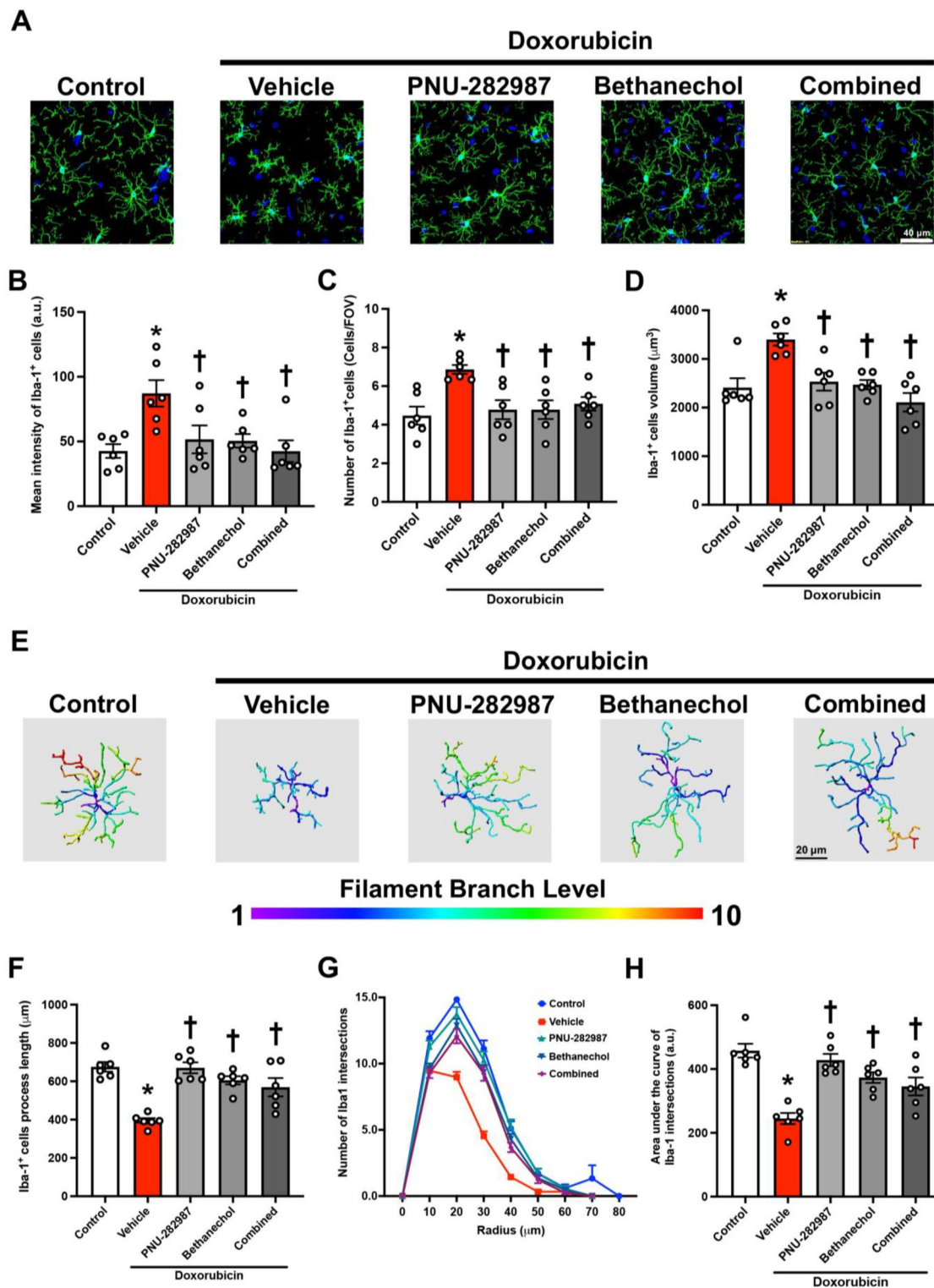


Fig. 4 The effects of $\alpha 7$ nAChR agonist and mAChR agonist on microglial morphology in rats with DOX-induced chemobrain. **A** Representative images of Iba-1 immunofluorescence under confocal microscopy at CA1 of the hippocampus. **B** The number of Iba-1-positive cells. **C** Mean intensity of Iba-1-positive cells. **D** Soma volume of Iba-1-positive cells. **E** Representative branch level of microglial

processes. **F** Process length of Iba-1-positive cells. **G** Microglial process complexity as the number of Iba-1-positive cell process intersections using Sholl analysis. **H** The representative area under the curve of Sholl analysis. Each dot represents the average value of two slices from one animal, $n=6$ rats per group; * $p < 0.05$ vs. control; † $p < 0.05$ vs. DOX + vehicle. FOV, field of vision

at levels comparable to those observed in the control group (Fig. 4A–H).

Fig. 5 A shows the reactivation of astrocytes in rat CA1 after DOX administration. Astrocytic activation in response to DOX was demonstrated by a significant increase in mean fluorescence intensity, number, and cell volume of GFAP+ cells (Fig. 5B–D). In addition, the length and complexity of processes analyzed by Sholl analysis of GFAP+ cells dramatically decreased in comparison to the controls (Fig. 5E–H). Importantly, treatment with either PNU-282987 or bethanechol significantly reduced GFAP immunofluorescence intensity, the number of GFAP+ cells, and soma volume of GFAP+ cells in rats treated with DOX (Fig. 5A–D). The filament analysis also revealed that the administration of PNU-282987 or bethanechol significantly increased the length and branching of astrocytic processes in DOX-treated rats (Fig. 5E–H). However, no synergistic effect of these drugs was observed in the combined groups (Fig. 5A–H). Conclusively, activation of α 7nAChR or mAChR using as the parasympathomimetic drugs was able to attenuate microglial and astrocytic activation in response to DOX administration.

The Activation of α 7nAChR and mAChR Improved Brain Mitochondrial Function and Suppressed Mitochondrial Fission in Rats with DOX-Induced Chemobrain

In this study, brain mitochondrial ROS-neutralizing ability was determined by co-incubation with H_2O_2 . The results demonstrated that DOX administration impaired mitochondrial ROS-neutralizing ability as indicated by a significant increase in the percentage change in mitochondrial ROS level after H_2O_2 stimulation relative to that observed in the control group (Fig. 6A). In comparison to the control rats, DOX-treated rats also exhibited a significant increase in H_2O_2 -stimulated membrane potential alterations, indicating mitochondrial membrane depolarization (Fig. 6B). Furthermore, DOX administration significantly decreased the absorbance of the isolated mitochondrial fraction in comparison to the control group, implying mitochondrial swelling in response to DOX treatment (Fig. 6B). PNU-282987, bethanechol, and the combined drugs had similar efficacy in preserving mitochondrial ROS-detoxifying capacity in DOX-treated rats (Fig. 6A–C).

The effects of the drugs on mitochondrial dynamics were subsequently investigated. Western blotting analysis revealed that administration of DOX significantly upregulated the expression of both mitochondrial fission- and fusion-related proteins as indicated by significant upregulation of the fission marker (phosphorylated Drp-1 at Ser616 relative to total Drp-1) and fusion factors including MFN-1, MFN-2, and OPA-1 (Fig. 6D–H). Noticeably, treatment

with PNU-282987, bethanechol, and the combined drugs equally attenuated excessive mitochondrial fission (Fig. 6D, E) in comparison to rats receiving DOX alone, while maintaining mitochondrial fusion as a compensatory mechanism (Fig. 6D, F–H). These findings demonstrated that PNU-282987, bethanechol, and the combined drugs improved brain mitochondrial ROS-detoxifying function and a balance of mitochondrial dynamics in rats with DOX-induced chemobrain.

The α 7nAChR Agonist and mAChR Agonist Mitigated Hippocampal Apoptosis in Rats with DOX-Induced Chemobrain

Western blotting analysis revealed that DOX administration diminished the cell survival pathways as evidenced by significant decreases in the expression of phosphoinositide 3-kinase (PI3K) and phosphorylation of protein kinase B (AKT) and ERK at Ser473 and Thr202/Tyr204, respectively (Fig. 7A–D). These contributed to a substantial reduction of Bcl-2 expression and an increased ratio of cleaved caspase-3 to caspase-3, observed in the hippocampal tissues of DOX-treated rats (Fig. 7A, E, F). Strikingly, pharmacological intervention with PNU-282987, bethanechol, or the combined drugs enhanced the expression of PI3K and the phosphorylation of AKT and ERK equally, resulting in a decrease in the expression of apoptotic markers (Fig. 7A–F). Taken together, this suggested that AChR agonists provided neuroprotection against DOX-mediated neuronal apoptosis in part via PI3K/AKT and ERK signaling pathways.

Long-Term Administration of DOX-Induced Hippocampal Pyroptosis and Necroptosis Which Were Diminished by Treatment with AChR Agonists

To support the hypothesis that DOX-induced chemobrain could lead to neuronal death via alternative forms of PCD, we further evaluated the pertinent proteins of each type of pro-inflammatory PCD including pyroptosis and necroptosis. Our results demonstrated that the expression of pyroptosis-related executioner protein, NOD-, LRR- and pyrin domain-containing protein 3 (NLRP3) inflammasomes, was markedly increased in DOX-treated rats (Fig. 8A, B). Consistently, higher levels of cleaved gasdermin D (GSDMD)/total GSDMD, and IL-1 β were evident in the hippocampal tissues of DOX-treated rats, further confirming the induction of pyroptosis following DOX administration. In addition to pyroptosis, the ratios of p-RIPK1^{ser166}/RIPK1, p-RIPK3^{ser232}/RIPK3, and p-MLKL^{ser358}/MLKL were also markedly increased, indicating necroptosis in the hippocampus of DOX-treated rats (Fig. 8A, E–G). In summary, we showed unique molecular findings supporting that DOX-mediated forms of PCD in the hippocampus

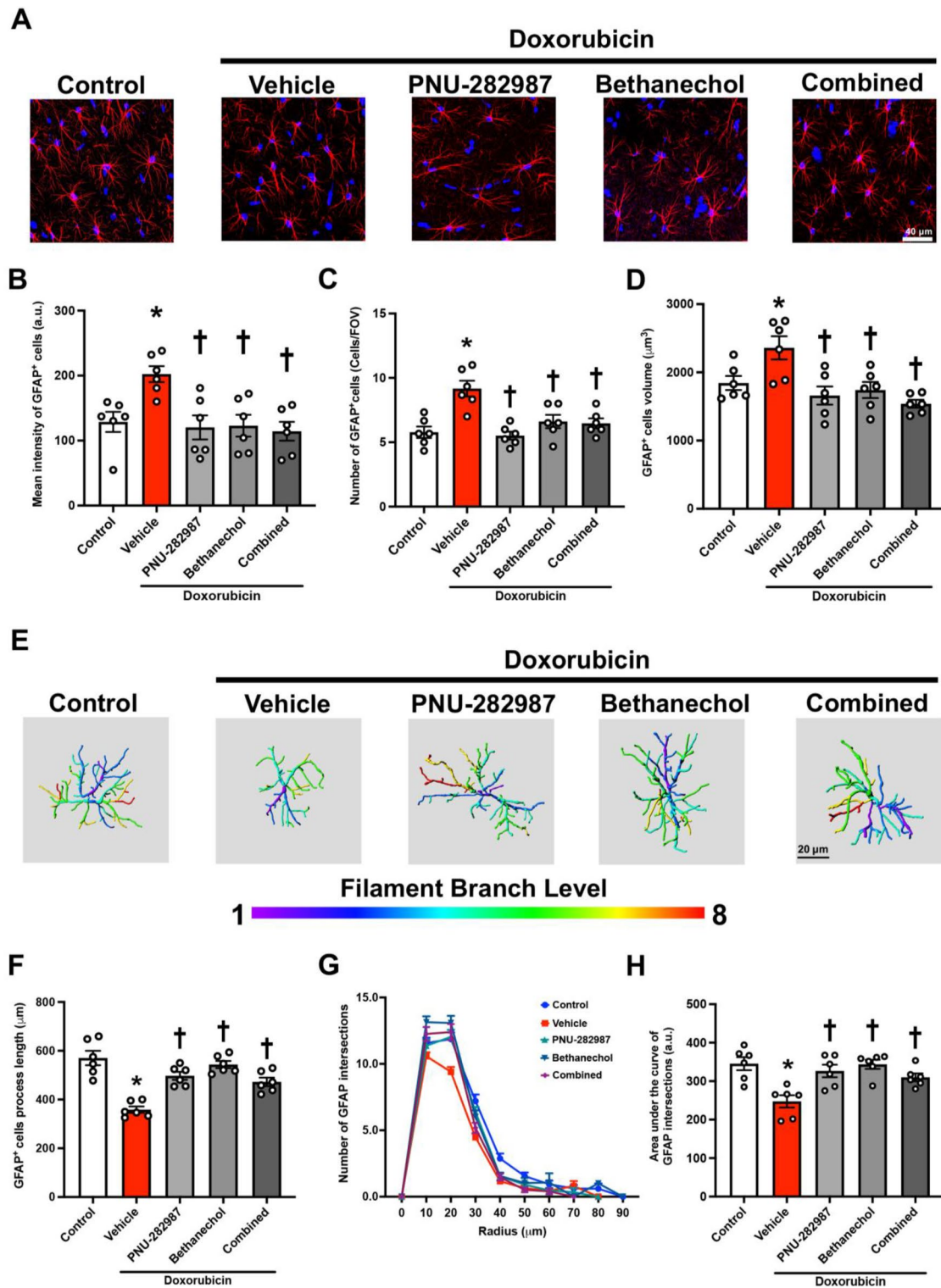


Fig. 5 The effects of an $\alpha 7$ nAChR agonist and mAChR agonist on astrocytic morphology in rats with DOX-induced chemobrain. **A** Representative images of GFAP immunofluorescence under confocal microscopy at CA1 of the hippocampus. **B** The number of GFAP-positive cells. **C** Mean intensity of GFAP-positive cells. **D** Soma volume of GFAP-positive cells. **E** Representative branch level

of astrocytic processes. **F** Process length of GFAP-positive cells. **G** Astrocytic process complexity as the number of GFAP-positive cell process intersections using Sholl analysis. **H** The representative area under the curve of Sholl analysis. Each dot represents the average value of two slices from one animal, $n=6$ rats per group; $*p < 0.05$ vs. control; $\dagger p < 0.05$ vs. DOX + vehicle. FOV, field of vision

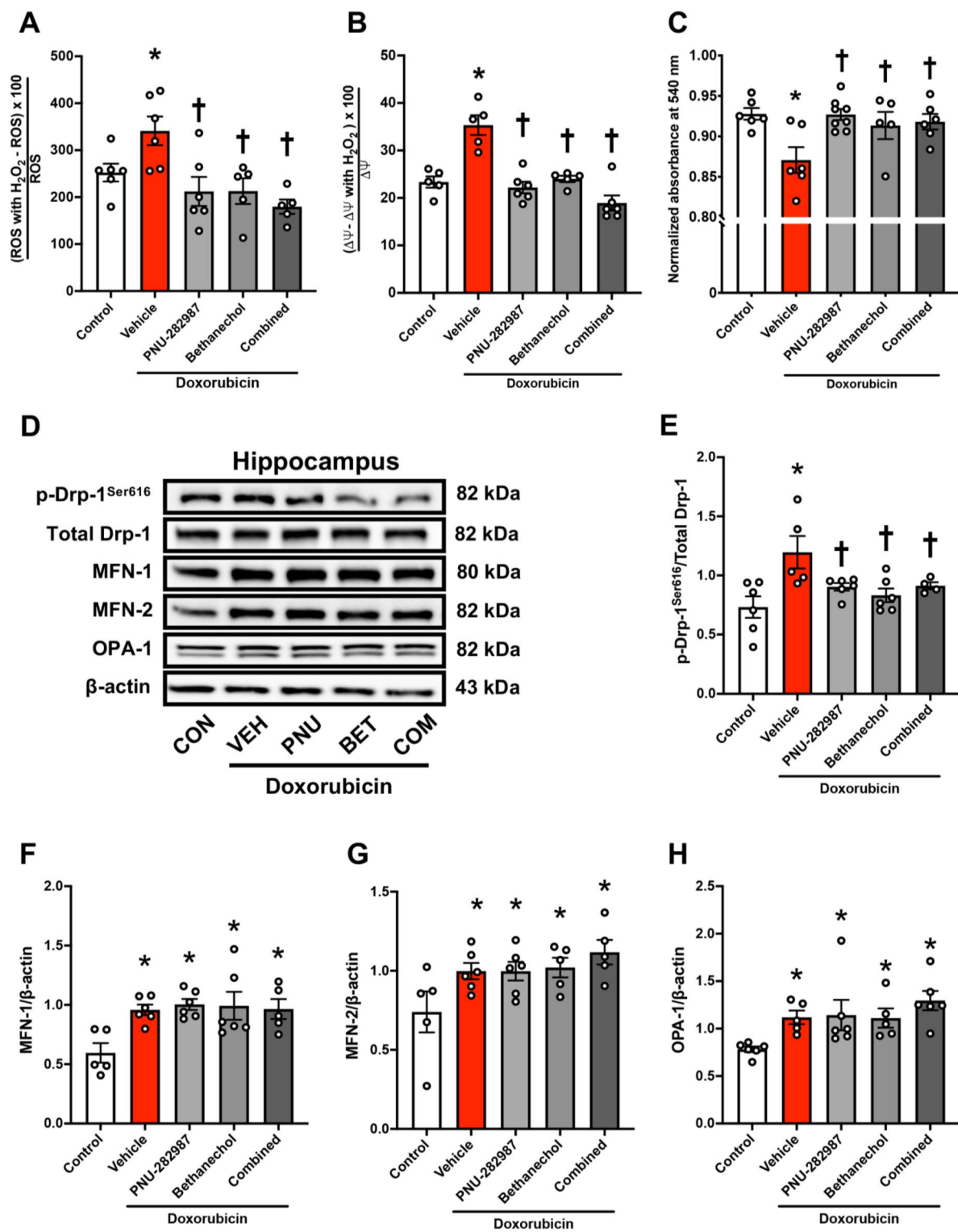
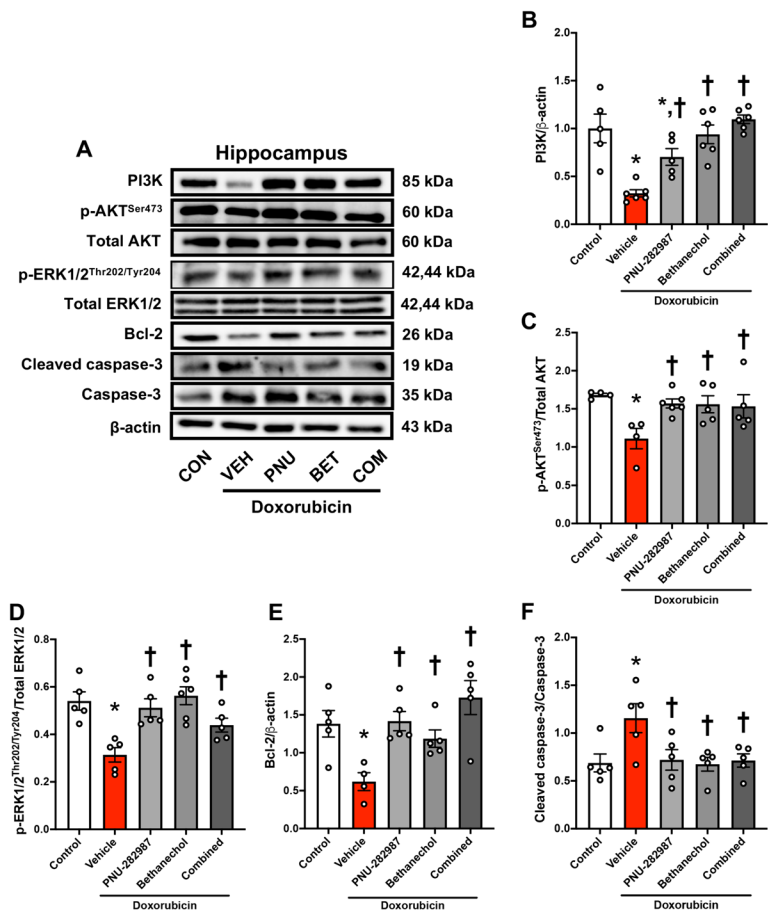


Fig. 6 The effects of an $\alpha 7$ nAChR agonist and mAChR agonist on mitochondrial function and dynamics in rats with DOX-induced chemobrain. **A** The percentage changes in ROS production after H₂O₂ stimulation. **B** Brain mitochondrial membrane potential changes after H₂O₂ stimulation. **C** Mitochondrial swelling as indicated by absorbance at a wavelength of 540 nm. **D** Representative western blot bands. **E** The expression ratio of p-Drp-1^{Ser616}/Drp-1. **F** MFN-1 protein expression. **G** MFN-2 protein expression. **H** OPA-1 protein expres-

sion; $n=5-8$ /group for mitochondrial function and $n=4-6$ /group for western blotting; * $p < 0.05$ vs. control; † $p < 0.05$ vs. Dox + vehicle (one-way ANOVA followed by an LSD post hoc test). $\Delta\Psi$, mitochondrial membrane potential; Dox, doxorubicin; Drp-1, dynamin-related protein-1; p-Drp-1^{Ser616}, phosphorylated dynamin-related protein-1 at serine 616; MFN-1, mitofusin 1; MFN-2, mitofusin 2; OPA-1, optic atrophy 1; ROS, reactive oxygen species

Fig. 7 The effects of an $\alpha 7$ nAChR agonist and mAChR agonist on hippocampal apoptosis in rats with DOX-induced chemobrain. **A** Representative western blot bands. **B** PI3K protein expression. **C** The expression ratio of p-AKT^{Ser473}/total AKT. **D** The expression ratio of p-ERK1/2^{Thr202/Tyr204}/total ERK1/2. **E** Bcl-2 protein expression. **F** The expression ratio of cleaved caspase-3/caspase-3; $n = 4-6$ /group; * $p < 0.05$ vs. control; † $p < 0.05$ vs. DOX + vehicle (one-way ANOVA followed by an LSD post hoc test). AKT, protein kinase B; PI3K, phosphoinositide 3-kinases



included apoptosis, necroptosis, and pyroptosis. Although treatment with AChR agonists did not alter the level of NLRP3 expression, they effectively reduced the expression IL-1 β and the cleavage of GSDMD which are initiators of the pyroptosis cascade (Fig. 8A–D). Treatment with PNU-282987 and the combined drugs suppressed the activation of the RIPK1-RIPK3-MLKL axis to the levels observed in the healthy controls (Fig. 8A–G). Concomitant treatment with bethanechol decreased the expression of p-RIPK1^{ser166}/RIPK1 and p-RIPK3^{ser232}/RIPK3 but did not reverse an increased ratio of p-MLKL^{ser358}/MLKL in DOX-treated rats (Fig. 8A, E–G). These results suggested that intervention with $\alpha 7$ nAChR or mAChR agonists effectively suppressed both pyroptosis and necroptosis in the hippocampus following DOX administration.

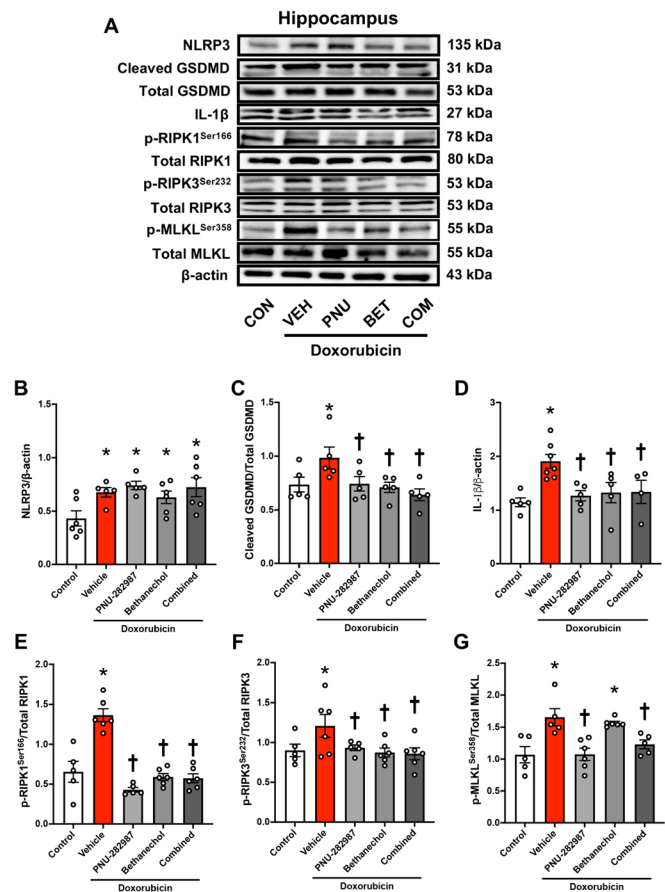
Discussion

The incidence of chemobrain has been attracting more attention in the medical field since it limits dosage administration or even leads to the inevitable termination of the treatments before completion of the regimen [50–52].

Comprehensive studies of the biological bases underlying chemobrain would contribute to the discovery of potential therapies to enhance the quality of life of cancer patients and survivors. This study mainly investigated the therapeutic efficacy of cholinergic activation using AChR agonists on the neuropathology of DOX-induced chemobrain. Our results underlined and extended the notion that DOX administration simultaneously induced multiple types of PCD including apoptosis, pyroptosis, and necroptosis in the hippocampus via upregulated inflammation, imbalance in mitochondrial homeostasis, loss of dendritic spine and BBB integrity, and hyperphosphorylation of Tau. Our study also provides novel insights into the neuroprotective impact of cholinergic activation as a promising therapeutic approach for treatment or even prevention of chemobrain. Treatment with AChR agonists in rats exposed to DOX effectively protected against the widespread aspects of neuropathology and mitigated several forms of PCD induced by DOX, contributing to an improvement of learning and memory.

Cholinergic receptors are broadly categorized into two main classes: the ionotropic nAChRs and the metabotropic mAChR. Both nAChRs and mAChR are expressed by

Fig. 8 The effects of an $\alpha 7$ nAChR agonist and mAChR agonist on hippocampal pyroptosis and necroptosis in rats with DOX-induced chemobrain. **A** Representative western blot bands. **B** NLRP3 protein expression. **C** Cleaved GSDMD/total GSDMD. **D** IL-1 β protein expression. **E** The expression ratio of p-RIPK1^{Ser166}/total RIPK1. **F** The expression ratio of p-RIPK3^{Ser232}/total RIPK3. **G** The expression ratio of p-MLKL^{Ser358}/total MLKL; $n = 4-6$ /group; * $p < 0.05$ vs. control; † $p < 0.05$ vs. DOX + vehicle (one-way ANOVA followed by an LSD post hoc test). GSDMD, gasdermin D; MLKL, mixed lineage kinase domain-like protein; NLRP3, NACHT, LRR, and PYD domain-containing protein 3; p-MLKL^{Ser358}, phosphorylation of MLKL at serine 358; p-RIPK1^{Ser166}, phosphorylation of RIPK1 at serine 166; p-RIPK3^{Ser232}, phosphorylation of RIPK3 at serine 232; RIPK1, receptor-interacting protein kinase 1; RIPK3, receptor-interacting protein kinase 3



neuronal and non-neuronal cells throughout the CNS and the peripheral nervous system [53, 54]. In the hippocampus, the most abundant nAChR subtype is $\alpha 7$ nAChR and it has been shown that the M1, M2, and M4 mAChRs are significantly expressed pre- or post-synaptically [55]. Neurophysiological evidence has established that the cholinergic nervous system is one of the key components participating in the maintenance of intact brain functions. It is thus unsurprising that abnormal alterations in the function of AChRs, particularly in the hippocampus, have been tightly orchestrated in the pathophysiology of AD [30]. In this line, a significant portion of hippocampal-dependent cognitive function is also acknowledged as one of the crucial cognitive domains affected by chemotherapy among cancer patients [56–58]. Previous *in vivo* studies demonstrated that DOX enhanced the activity of acetylcholinesterase (AChE) and impeded the synthesis of acetylcholine (ACh) by lowering choline levels and suppressing choline acetyltransferase activity, thereby impairing cognitive function in rodents [59, 60]. Collectively, these studies accentuated the cholinergic disturbances as significant contributory components in the pathophysiological cascade of DOX-induced chemobrain. Therefore, in this study, the impact of chemotherapeutic DOX and AChR agonists as interventions on cognitive performance

was investigated using a modified cognitive testing procedure consisting of NOLT and NORT. The NOLT was followed by the NORT within a 24-h resting period in order to impose a cognitive load on both long-term spatial and working memories, which are regulated by hippocampal activity [61]. DOX-treated rats exhibited an inability to recognize a new location or object in NOLT and NORT, respectively, reflecting a deficit in hippocampal-dependent learning and memory. Interestingly, we demonstrated that concomitant treatment with either an $\alpha 7$ nAChR or mAChR agonist diminished DOX-induced hippocampal-dependent cognitive impairment as represented by increased preference indexes in NOLT and NORT. Consistent with these findings, we previously demonstrated that intervention with AChE inhibitor donepezil showed prominent cognitive benefits in preservation of brain function in rats with DOX-induced chemobrain which was similar to the cognitive outcomes observed in DOX-treated rats receiving AChR agonists [21]. Hence, our results further suggest that the elevated level of ACh in response to donepezil treatment possibly exerted neuroprotection against DOX-mediated neurotoxicity via the activation of either $\alpha 7$ nAChR or mAChR. Together, these data comprehensively spotlighted the neuroprotective roles of AChR activation in preservation

of hippocampal-dependent cognitive function in a rat model of DOX-induced chemobrain.

Our investigation discovered reductions in dendritic spine density and volume in the hippocampal CA1 region as well as a decline in post-synaptic protein marker PSD-95 following DOX administration, implying weakening synaptic integrity. Unfortunately, the mechanism underlying the reduction of synaptic structure after chemotherapy is still largely unknown. Of significance, dendritic spines contain a substantial number of mitochondria, causing this neuronal compartment to be the most vulnerable to oxidative stress [62]. Therefore, DOX-mediated oxidative damage to these synaptosomal mitochondria possibly leads to a loss of synaptic integrity, which has been considered an early pathological manifestation of neurodegeneration [62]. In addition to oxidative stress, a previous study showed that inflammatory mediators secreted from activated microglia diminished the modulatory signals of brain-derived neurotrophic factor (BDNF) and elicited excitotoxicity, resulting in dendritic spine damage [63]. Remarkably, pharmacological intervention with all AChR agonists sustained all aforementioned synaptic parameters to equivalent levels observed in the control groups. We therefore speculated that cholinergic activation of either $\alpha 7$ nAChR or mAChR preserved synaptic integrity in rats with DOX-induced chemobrain via amelioration of neuroinflammation and brain mitochondrial ROS-neutralizing function.

There is a common consensus that neuroinflammation is the main cause of the pathogenesis of DOX-induced chemobrain [13]. A previous study demonstrated that microglial depletion with the colony-stimulating factor 1 receptor (CSF1R) inhibitor entirely abrogated neuroinflammation and cognitive decline in mice receiving DOX, further confirming the significant involvement of microglial activation as the central player in the perpetuation of DOX-induced chemobrain [17]. Similarly, we found an upregulation of the expression of pro-inflammatory cytokines including TNF- α and IL-1 β as well as the phosphorylation of NF- κ B in the hippocampus of rats receiving DOX. An anti-inflammatory cytokine IL-10 and the phosphorylation of STAT3 were also downregulated following DOX administration. Furthermore, the 3D morphological-based quantitative analysis demonstrated that microglia and astrocytes in the CA1 region were prone to polarize into pro-inflammatory, neurotoxic phenotypes as depicted by an amoeboid-like shaped morphology. Microglia also presented with decreased process length and complexity in response to DOX treatment, displaying transcriptomic alterations that indicate a neurodegenerative microglia phenotype largely approximating that of the stage 1 disease-associated microglia (DAM) [16]. Collectively, these data indicated the rigor of DOX-mediated neuroinflammation. Bidirectional communication between the cholinergic system and the immune system in the CNS has been

identified as indicated by common receptors and ligands are expressed in cells of both systems [64, 65]. Using cholinergic activation as a therapeutic strategy in the current study, long-term treatment with PNU-282987, bethanechol, or the two drugs combined reversed pro-inflammatory profiles and altered microglial and astrocytic morphology in the CA1 region of DOX-treated rats, indicating the anti-inflammatory effect of AChR activation against DOX toxicity. Notably, PNU-282987, but not bethanechol, upregulated the phosphorylation of STAT3 at Tyr705, implying that $\alpha 7$ nAChR activation conveyed anti-inflammatory signaling partly via the induction of the STAT3 pathway. Following this line of thought, $\alpha 7$ nAChR has also previously been identified as a potent mediator of anti-inflammatory pathways via the activation of the Jak2/STAT3 pathway to facilitate the blockage of NF- κ B translocation, further suppressing the production of pro-inflammatory cytokines [65, 66]. Treatment with selective $\alpha 7$ nAChR agonists ameliorated neuroinflammation and cytokine production via attenuation of microglia and astrocyte reactivation [67–70]. In the present study, even though treatment with the mAChR agonist bethanechol did not alter the activation of STAT3, a decline in the pro-inflammatory cytokines was still observed, suggesting the possibility that mAChR activation regulates anti-inflammatory processes via other alternative pathways. A previous study demonstrated that selective optogenetic stimulation of cholinergic neurons caused the significant expression of M1 mAChR in the basal forebrain or M1 mAChR agonist therapy effectively reducing the level of serum TNF α during endotoxemia [37, 71]. Additionally, a non-selective mAChR agonist, oxotremorine, was shown to significantly hamper the expression of pro-inflammatory cytokines in the hippocampus of rats that underwent chronic restraint stress [72]. Therefore, it is possible that mAChR activation regulates anti-inflammatory effects in DOX-treated rats mainly via M1 mAChR signaling. However, further investigations using genetic modification or selective agonists/antagonists are needed to identify the specific receptors and mechanisms.

In addition to neuroinflammation, a substantial number of previous studies have reported brain mitochondrial abnormalities following systemic administration of DOX [15, 18, 21, 73, 74]. Prior works demonstrated that DOX administration in rodents impaired mitochondrial oxidative regulation and calcium homeostasis in the brain, ultimately leading to brain oxidative burst and impairment in hippocampal-dependent learning and memory [15, 21]. We recently demonstrated that Dox treatment caused a fluctuation in brain mitochondrial dynamics by promoting both fusion-related protein expression and phosphorylation of the fission protein Drp-1 [18]. Although the precise mechanism remains obscure, it has been suggested that excessive oxidative stress following DOX treatment is a key element driving the upregulated phosphorylation of the fission-related

protein Drp-1 [18, 21]. Inhibition of mitochondrial fission has the capacity to rebalance these changes and improve cognitive function in rats treated with DOX [18]. Likewise, activation of either an $\alpha 7$ nAChR or mAChR agonist could also be beneficial in protecting brain function against DOX-induced chemobrain through these mitochondrial protection processes. It is conceivable that activation of AChRs using their agonists provides anti-oxidant capacity, leading to a rebalance of mitochondrial dynamics in the hippocampus. This is corroborated by the fact that activation of $\alpha 7$ nAChR induced the upregulation of the canonical Nrf2/HO-1 anti-oxidant pathway in both microglia and astrocytes [68, 70]. In addition, oxotremorine treatment, a non-selective mAChR agonist, was capable of mitigating oxidative damage and mitochondrial abnormalities in differentiated SH-SY5Y cells exposed to amyloid- β [75]. Insights into these subcellular mechanisms strongly illustrate the mitoprotective efficacy of cholinergic activation against DOX-induced chemobrain.

Post-translational modifications of Tau, particularly hyperphosphorylation of Tau at Thr181, have been broadly shown to regulate a spectrum of neurodegenerative diseases. Interestingly, treatment with $\alpha 7$ nAChR or mAChR agonists effectively attenuated the hyperphosphorylation of Tau at Thr181 in the hippocampus following DOX treatment. The phosphorylated Thr181 residues can lead to microtubule instability as it is complicated by the binding kinetics of the Tau microtubule, resulting in the formation of neurofibrillary tangles (NFTs) [76]. In depth, we demonstrated that activation of $\alpha 7$ nAChR or mAChR induced the activation of their downstream signaling kinases including PI3K, AKT, and ERK1/2. Although the ionotropic activity of $\alpha 7$ nAChR is a pronounced property of neurons, the metabotropic ways are prevalent downstream of $\alpha 7$ nAChR activation in non-neuronal cells. It has been reported that $\alpha 7$ nAChR mediates neuroprotective effects through the involvement of various intracellular signaling pathways including PI3K/AKT [77]. Activation of M1 and M4 mAChRs is also associated with signal transduction via the engagement of PI3K and AKT [78]. Previous studies have demonstrated that AKT inhibited the activity of GSK3 β , a kinase significantly responsible for Tau hyperphosphorylation in AD pathology [79, 80]. Consistently, activation of $\alpha 7$ nAChR with PNU-282987 led to increased phosphorylation of AKT and GSK3 β and a subsequent decline in phosphorylated Tau in hypothalamic neurons treated with a conditioned medium obtained from microglial cells previously stimulated with LPS [81]. The M1 mAChR agonist showed a protective effect on cognition by mitigating the hyperphosphorylated Tau and the number of neurons containing aggregated Tau [82]. From these results, we suggest that activation of $\alpha 7$ nAChR or M1 and M4 mAChRs prevented hyperphosphorylation of Tau in the hippocampus of DOX-treated rats possibly via the activation of the PI3K/AKT/GSK3 β axis.

Aberrant activation of PCD in the neuronal cell population is a principal characteristic of pathologies involved in neurodegenerative diseases, culminating in detrimental loss of neuronal cells and cognitive deficit, respectively. As noted above, the deleterious effects of DOX on the CNS potentially orchestrate neuronal injury, ultimately leading to neuronal cell death. The importance of the present study is that DOX simultaneously induced several types of PCD including apoptosis, pyroptosis, and necroptosis. A series of extensive studies have comprehensively indicated that mitochondrial dysfunction is a key initiator of neuronal apoptosis following DOX administration [15, 74, 83]. We have also previously demonstrated that DOX administration provoked neuronal death in the hippocampus partly through necroptosis as affirmed by upregulated phosphorylation of RIPK1, RIPK3, and MLKL. It is therefore conceivable that the elevation of TNF- α level in response to DOX could induce the activation of the RIPK1–RIPK3–MLKL pathway via binding with tumor necrosis factor receptor 1 (TNFR1), eventually resulting in the assembly of necrosomes and subsequent necroptosis-mediated cell membrane rupture. Interestingly, concomitant intervention with either $\alpha 7$ nAChR or mAChR agonists exerted influential anti-apoptotic, necroptotic, and pyroptotic properties in rats with DOX-induced chemobrain, indicating activation of AChRs protects against PCD following DOX administration in the brain by preventing mitochondrial dysfunction and neuroinflammation. Indeed, it has been previously described that the stimulation of $\alpha 7$ nAChR initiates the survival PI3K/AKT/Bcl-2 pathway which may have contributed to the neuroprotection against DOX toxicity observed in the current study [84]. Similarly, it is known that mAChR inhibited apoptosis through the activation of PI3K and its downstream targets AKT and ERK1/2 [85]. Nonetheless, the direct anti-necroptotic effects of cholinergic activation in the brain are still poorly understood. We suggest that cholinergic anti-inflammatory effects could contribute to the suppression of TNF- α production, thereby preventing TNFR1 from initiating the necroptosis cascade in response to DOX administration. To our knowledge, this present study demonstrated for the first time that DOX monotherapy upregulated the expression of NLRP3, cleaved GSDMD, and IL-1 β in the hippocampus, further indicating the existence of pyroptosis in response to DOX treatment. In correlation with the previous study, the effects of the combined therapy of cyclophosphamide and DOX have been shown to be associated with NLRP3-mediated oxidative stress and a debilitating neuroinflammation in the hippocampus [86]. However, further investigation is needed to determine whether damage-associated molecular patterns (DAMPs) or pathogen-associated molecular patterns (PAMPs) are responsible for the initiation of pyroptotic processes in DOX-induced chemobrain. Even though the molecular mechanism has not yet been identified, a previous study demonstrated that treatment with ACh or the $\alpha 7$ nAChR

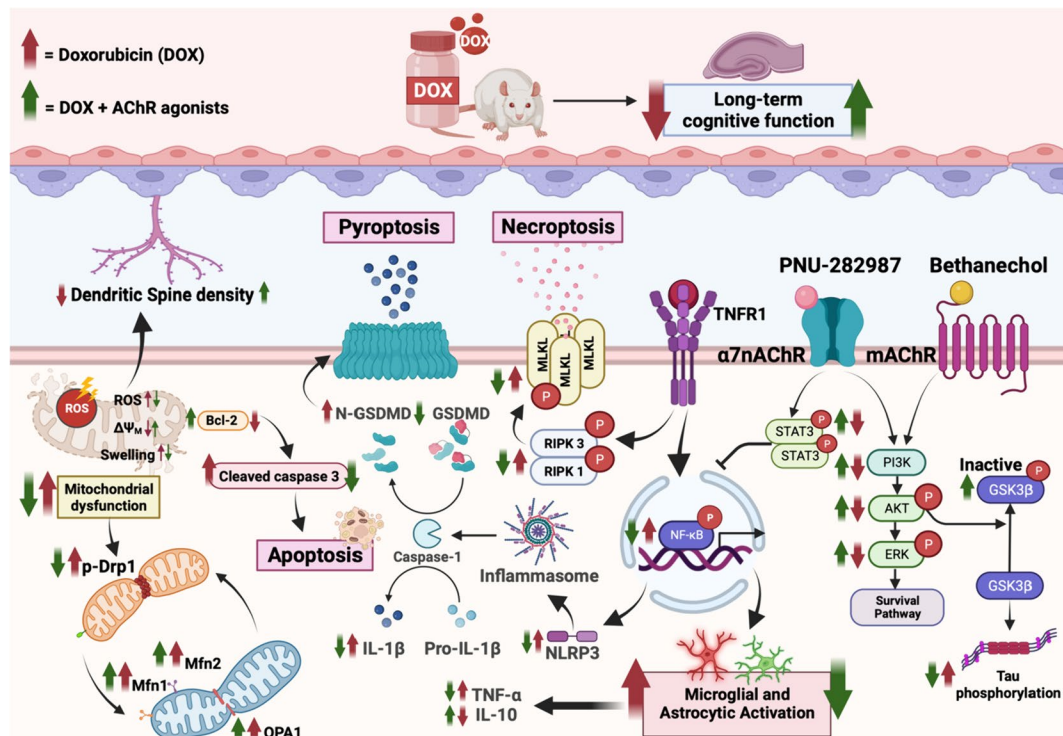


Fig. 9 Schematic representation of the proposed mechanisms of AChR agonists against DOX-induced chemobrain. AChR agonists preserved long-term memory against DOX toxicity by reducing neuroinflammation and glial activation, restoring normal mitochondrial function and dynamics, and mitigating Tau hyperphosphorylation and

various forms of programmed cell death including apoptosis, pyroptosis, and necroptosis. The effects of DOX administration in rats are denoted by red arrows, while the effects of AChR agonists in DOX-treated rats are represented by green arrows

agonist GTS-2 inhibited internalization of extracellular high mobility group 1 protein (HMGB1), a potential initiator of pyroptosis, in cultured macrophages [87]. Additionally, the $\alpha 7$ nAChR agonist also mimicked the benefits of vagus nerve stimulation by inhibiting neuronal pyroptosis after cerebral ischemia/reperfusion injury [88]. Therefore, we suggest that cholinergic activation possibly inhibited DOX-mediated pyroptosis via inhibition of DAMP or PAMPs internalization and the cholinergic anti-inflammatory pathway.

Surprisingly, the synergistic effects of the combined treatment were not observed in the DOX-induced chemobrain in the present study. It is possible that monotherapy with either $\alpha 7$ nAChR agonist or mAChR agonist already reached the maximal benefits with regard to DOX-induced chemobrain. It is conceivable that the systemic activation of either $\alpha 7$ nAChR or mAChR conveys the same common pathways to exert neuroprotection against DOX-induced chemobrain. Therefore, when the shared downstream pathways of these AChRs have already been thoroughly stimulated, the synergistic effects would not be discernible. Collectively, our study enhances our understanding of multiple types of PCD induced by chemotherapy, including apoptosis, necroptosis, and pyroptosis in the hippocampus, further gaining a comprehensive understanding of the molecular pathophysiology of

chemobrain. These insights provide promising targets for the further development of effective interventions to treat chemobrain in the future. Furthermore, our research emphasizes the specific protective function mediated by each AChR receptor, thus providing in-depth neuroprotective mechanisms of AChR agonists that can be used as possible treatment options to alleviate neurological complications in cancer patients receiving chemotherapy, as well as for other neurodegenerative diseases. The proposed mechanisms in which $\alpha 7$ nAChR and mAChR agonists exerted neuroprotective effects against DOX-induced chemobrain are illustrated in Fig. 9.

Conclusion

Our study demonstrated that cholinergic activation exerted neuroprotective effects in experimental rats with DOX-induced chemobrain through attenuation of neuroinflammation and glial activation, restoration of mitochondrial function and dynamics, and mitigation of several types of PCD. The current study substantiates the potential therapeutic advantages of parasympathetic therapy utilizing AChR agonists as a promising novel therapy to protect cancer patients against neurological sequelae.

Supplementary Information The online version contains supplementary material available at <https://doi.org/10.1007/s12035-024-04145-0>.

Author Contribution Conceptualization: Benjamin Ongnok, Nanthip Prathumsap, Nipon Chattipakorn, and Siriporn C Chattipakorn. Investigation: Benjamin Ongnok, Nanthip Prathumsap, Titikorn Chunchai, Patcharapong Pantiya, Busarin Arunsak. Formal analysis: Benjamin Ongnok; Supervision: Nipon Chattipakorn and Siriporn C Chattipakorn. Writing — original draft: Benjamin Ongnok. Writing — review and editing: Siriporn C Chattipakorn. All authors approved the final manuscript.

Funding This work was supported by the Distinguished Research Professor grant from the National Research Council of Thailand (N42A660301 to SCC); the Royal Golden Jubilee Ph.D. program (PHD/0106/2561 BO&SCC); the Research Chair Grant from the National Research Council of Thailand (NC); and a Chiang Mai University Excellence Center Award (NC).

Data Availability The datasets used and/or analyzed during the current study are available from the corresponding author upon reasonable request.

Declarations

Ethics Approval All experimental procedures were performed under the protocol approved by the Institutional Animal Care and Use Committee (IACUC) of Chiang Mai University (permit no. 2563/RT-0012) and were carried out in accordance with the recommendations of NIH guidelines (Guide for the Care and Use of Laboratory Animals).

Consent to Participate Not applicable.

Consent for Publication Not applicable.

Competing Interests The authors declare no competing interests.

References

- Miller KD, Siegel RL, Lin CC, Mariotto AB, Kramer JL, Rowland JH, Stein KD, Alteri R (2016) Jemal A (2016) Cancer treatment and survivorship statistics. *CA Cancer J Clin* 66(4):271–289. <https://doi.org/10.3322/caac.21349>
- Fosså SD, de Wit R, Roberts JT, Wilkinson PM, de Mulder PH, Mead GM, Cook P, de Prijck L et al (2003) Quality of life in good prognosis patients with metastatic germ cell cancer: a prospective study of the European Organization for Research and Treatment of Cancer Genitourinary Group/Medical Research Council Testicular Cancer Study Group (30941/TE20). *J Clin Oncol* 21(6):1107–1118. <https://doi.org/10.1200/jco.2003.02.075>
- Wefel JS, Saleeba AK, Buzdar AU, Meyers CA (2010) Acute and late onset cognitive dysfunction associated with chemotherapy in women with breast cancer. *Cancer* 116(14):3348–3356. <https://doi.org/10.1002/cncr.25098>
- Schagen SB, Muller MJ, Boogerd W, Rosenbrand RM, van Rhijn D, Rodenhuis S, van Dam FSAM (2002) Late effects of adjuvant chemotherapy on cognitive function: a follow-up study in breast cancer patients. *Ann Oncol* 13(9):1387–1397. <https://doi.org/10.1093/annonc/mdf241>
- Wefel JS, Schagen SB (2012) Chemotherapy-related cognitive dysfunction. *Curr Neurol Neurosci Rep* 12(3):267–275. <https://doi.org/10.1007/s11910-012-0264-9>
- Stewart A, Bielajew C, Collins B, Parkinson M, Tomiak E (2006) A meta-analysis of the neuropsychological effects of adjuvant chemotherapy treatment in women treated for breast cancer. *Clin Neuropsychol* 20(1):76–89. <https://doi.org/10.1080/138540491005875>
- Jim HS, Phillips KM, Chait S, Faul LA, Popa MA, Lee YH, Husain MG, Jacobsen PB et al (2012) Meta-analysis of cognitive functioning in breast cancer survivors previously treated with standard-dose chemotherapy. *J Clin Oncol* 30(29):3578–3587. <https://doi.org/10.1200/jco.2011.39.5640>
- Lindner OC, Phillips B, McCabe MG, Mayes A, Wearden A, Varese F, Talmi D (2014) A meta-analysis of cognitive impairment following adult cancer chemotherapy. *Neuropsychology* 28(5):726–740. <https://doi.org/10.1037/neu0000064>
- Hodgson KD, Hutchinson AD, Wilson CJ, Nettelbeck T (2013) A meta-analysis of the effects of chemotherapy on cognition in patients with cancer. *Cancer Treat Rev* 39(3):297–304. <https://doi.org/10.1016/j.ctrv.2012.11.001>
- Pendergrass JC, Targum SD, Harrison JE (2018) Cognitive impairment associated with cancer: a brief review. *Innov Clin Neurosci* 15(1–2):36–44
- Carvalho C, Santos RX, Cardoso S, Correia S, Oliveira PJ, Santos MS, Moreira PI (2009) Doxorubicin: the good, the bad and the ugly effect. *Curr Med Chem* 16(25):3267–3285. <https://doi.org/10.2174/092986709788803312>
- Eide S, Feng ZP (2020) Doxorubicin chemotherapy-induced “chemo-brain”: Meta-analysis. *Eur J Pharmacol* 881:173078. <https://doi.org/10.1016/j.ejphar.2020.173078>
- Ongnok B, Chattipakorn N, Chattipakorn SC (2020) Doxorubicin and cisplatin induced cognitive impairment: the possible mechanisms and interventions. *Exp Neuro* 324:113118. <https://doi.org/10.1016/j.expneurol.2019.113118>
- Nguyen LD, Ehrlich BE (2020) Cellular mechanisms and treatments for chemobrain: insight from aging and neurodegenerative diseases. *EMBO Mol Med* 12(6):e12075. <https://doi.org/10.15252/emmm.202012075>
- Park HS, Kim CJ, Kwak HB, No MH, Heo JW, Kim TW (2018) Physical exercise prevents cognitive impairment by enhancing hippocampal neuroplasticity and mitochondrial function in doxorubicin-induced chemobrain. *Neuropharmacology* 133:451–461. <https://doi.org/10.1016/j.neuropharm.2018.02.013>
- McAlpin BR, Mahalingam R, Singh AK, Dharmaraj S, Chrisikou TT, Boukelmoun N, Kavelaars A, Heijnen CJ (2022) HDAC6 inhibition reverses long-term doxorubicin-induced cognitive dysfunction by restoring microglia homeostasis and synaptic integrity. *Theranostics* 12(2):603–619. <https://doi.org/10.7150/thno.67410>
- Allen BD, Apodaca LA, Syage AR, Markarian M, Baddour AAD, Minasyan H, Alikhani L, Lu C et al (2019) Attenuation of neuroinflammation reverses adriamycin-induced cognitive impairments. *Acta Neuropathol Commun* 7(1):186. <https://doi.org/10.1186/s40478-019-0838-8>
- Ongnok B, Manechote C, Chunchai T, Pantiya P, Arunsak B, Nawara W, Chattipakorn N, Chattipakorn SC (2022) Modulation of mitochondrial dynamics rescues cognitive function in rats with “doxorubicin-induced chemobrain” via mitigation of mitochondrial dysfunction and neuroinflammation. *Febs j* 289(20):6435–6455. <https://doi.org/10.1111/febs.16474>
- Cui J, Zhao S, Li Y, Zhang D, Wang B, Xie J, Wang J (2021) Regulated cell death: discovery, features and implications for neurodegenerative diseases. *Cell Commun Signal* 19(1):120. <https://doi.org/10.1186/s12964-021-00799-8>
- Goel P, Chakrabarti S, Goel K, Bhutani K, Chopra T, Bali S (2022) Neuronal cell death mechanisms in Alzheimer’s disease: an insight. *Front Mol Neurosci* 15:937133. <https://doi.org/10.3389/fnmol.2022.937133>
- Ongnok B, Khuanjing T, Chunchai T, Pantiya P, Kerdphoo S, Arunsak B, Nawara W, Jaiwongkam T et al (2021) Donepezil

- increased phosphorylation of Akt substrates and loss and altered distribution of Akt and PTEN are features of Alzheimer's disease pathology. *J Neurochem* 93(1):105–117. <https://doi.org/10.1111/j.1471-4159.2004.02949.x>
81. Amaral CLD, Martins ÍCA, Veras ACC, Simabuco FM, Ross MG, Desai M, Ignácio-Souza LM, Milanski M et al (2022) Activation of the $\alpha 7$ nicotinic acetylcholine receptor prevents against microglial-induced inflammation and insulin resistance in hypothalamic neuronal cells. *Cells* 11:14. <https://doi.org/10.3390/cells11142195>
 82. Fisher A, Pittel Z, Haring R, Bar-Ner N, Kliger-Spatz M, Natan N, Egozi I, Sonogo H et al (2003) M1 muscarinic agonists can modulate some of the hallmarks in Alzheimer's disease: implications in future therapy. *J Mol Neurosci* 20(3):349–356. <https://doi.org/10.1385/jmn:20:3:349>
 83. Tangpong J, Miriyala S, Noel T, Sinthupibulyakit C, Jungsuwadee P, Clair D (2010) Doxorubicin-induced central nervous system toxicity and protection by xanthone derivative of *Garcinia Mangostana*. *Neuroscience* 175:292–299. <https://doi.org/10.1016/j.neuroscience.2010.11.007>
 84. Wallace TL, Porter RH (2011) Targeting the nicotinic $\alpha 7$ acetylcholine receptor to enhance cognition in disease. *Biochem Pharmacol* 82(8):891–903. <https://doi.org/10.1016/j.bcp.2011.06.034>
 85. Marte BM, Downward J (1997) PKB/Akt: connecting phosphoinositide 3-kinase to cell survival and beyond. *Trends Biochem Sci* 22(9):355–358. [https://doi.org/10.1016/s0968-0004\(97\)01097-9](https://doi.org/10.1016/s0968-0004(97)01097-9)
 86. Jia L, Zhou Y, Ma L, Li W, Chan C, Zhang S, Zhao Y (2023) Inhibition of NLRP3 alleviated chemotherapy-induced cognitive impairment in rats. *Neurosci Lett* 793:136975. <https://doi.org/10.1016/j.neulet.2022.136975>
 87. Yang H, Liu H, Zeng Q, Imperato GH, Addorisio ME, Li J, He M, Cheng KF et al (2019) Inhibition of HMGB1/RAGE-mediated endocytosis by HMGB1 antagonist box A, anti-HMGB1 antibodies, and cholinergic agonists suppresses inflammation. *Mol Med* 25(1):13. <https://doi.org/10.1186/s10020-019-0081-6>
 88. Tang H, Li J, Zhou Q, Li S, Xie C, Niu L, Ma J, Li C (2022) Vagus nerve stimulation alleviated cerebral ischemia and reperfusion injury in rats by inhibiting pyroptosis via $\alpha 7$ nicotinic acetylcholine receptor. *Cell Death Discov* 8(1):54. <https://doi.org/10.1038/s41420-022-00852-6>

Publisher's Note Springer Nature remains neutral with regard to jurisdictional claims in published maps and institutional affiliations.

Springer Nature or its licensor (e.g. a society or other partner) holds exclusive rights to this article under a publishing agreement with the author(s) or other rightsholder(s); author self-archiving of the accepted manuscript version of this article is solely governed by the terms of such publishing agreement and applicable law.